

Mechanistic Insight into Asymmetric Hetero-Michael Addition of α,β -Unsaturated Carboxylic Acids Catalyzed by Multifunctional Thioureas

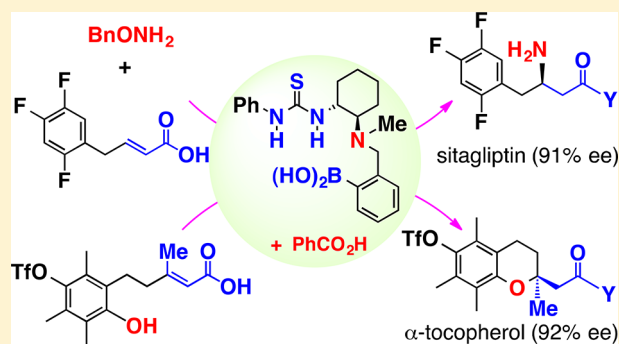
Noboru Hayama,[†] Ryuta Kuramoto,[†] Tamás Földes,[‡] Kazuya Nishibayashi,[†] Yusuke Kobayashi,[†] Imre Pápai,^{*,‡} and Yoshiji Takemoto^{*,†}

[†]Graduate School of Pharmaceutical Sciences, Kyoto University, Yoshida, Sakyo-ku, Kyoto 606-8501, Japan

[‡]Institute of Organic Chemistry, Research Centre for Natural Sciences, Hungarian Academy of Sciences, Magyar tudósok körútja 2, H-1117 Budapest, Hungary

Supporting Information

ABSTRACT: Carboxylic acids and their corresponding carboxylate anions are generally utilized as Brønsted acids/bases and oxygen nucleophiles in organic synthesis. However, a few asymmetric reactions have used carboxylic acids as electrophiles. Although chiral thioureas bearing both arylboronic acid and tertiary amine were found to promote the aza-Michael addition of BnONH_2 to α,β -unsaturated carboxylic acids with moderate to good enantioselectivities, the reaction mechanism remains to be clarified. Detailed investigation of the reaction using spectroscopic analysis and kinetic studies identified tetrahedral borate complexes, comprising two carboxylate anions, as reaction intermediates. We realized a dramatic improvement in product enantioselectivity with the addition of 1 equiv of benzoic acid. In this aza-Michael reaction, the boronic acid not only activates the carboxylate ligand as a Lewis acid, together with the thiourea NH-protons, but also functions as a Brønsted base through a benzoyloxy nucleophile to activate the nucleophile. Moreover, molecular sieves were found to play an important role in generating the ternary borate complexes, which were crucial for obtaining high enantioselectivity as demonstrated by DFT calculations. We also designed a new thiourea catalyst for the intramolecular oxa-Michael addition to suppress another catalytic pathway via a binary borate complex using steric hindrance between the catalyst and substrate. Finally, to demonstrate the synthetic versatility of both hetero-Michael additions, we used them to accomplish the asymmetric synthesis of key intermediates in pharmaceutically important molecules, including sitagliptin and α -tocopherol.

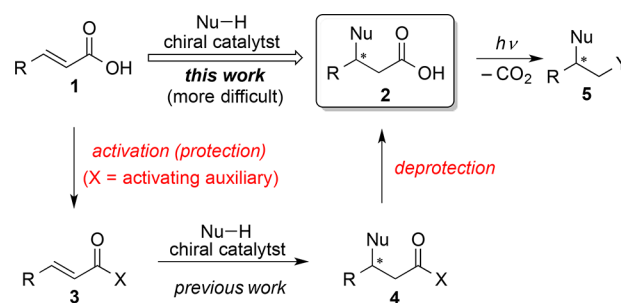


INTRODUCTION

Exploiting powerful catalytic methodologies for the asymmetric syntheses of natural products and potential pharmaceuticals from simple materials without using protecting and activating groups is the ultimate goal of synthetic organic chemistry.¹ Catalytic asymmetric Michael additions have attracted much attention regarding their atom economy and green credentials. Accordingly, an increasing number of catalytic asymmetric reactions using activated carboxylic acid derivatives² have been developed and utilized for the construction of complex molecules.³ However, new design concepts for chiral multifunctional catalysts capable of significantly activating substrates and nucleophiles are still needed, especially for reactions using less reactive Michael acceptors, such as α,β -unsaturated esters, amides, and carboxylic acids.⁴ The direct Michael addition to α,β -unsaturated carboxylic acids **1** is particularly challenging⁵ because carboxylic acids generally form inert salts with basic nucleophiles, and the resulting carboxylate anions are known to be the least reactive electrophiles among carboxylic acid derivatives for both the 1,2- and 1,4-additions. Therefore, so

far, only a few such methods, using enzymes such as ammonia lyases and aminomutases, have been reported,⁶ despite the versatile utilities of adducts **2** (Scheme 1).⁷ At present, no efficient synthetic tools exist for activating free carboxyl groups

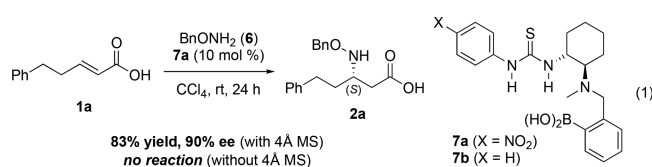
Scheme 1. Concept of this Work



Received: July 16, 2018

in a direct catalytic manner. Such a tool would mean that both the protection of **1** to activated adducts **3** using 1 equiv of activating auxiliaries (*X*) and the deprotection of Michael adducts **4** to the corresponding carboxylic acids **2** would not be necessary. This would allow desired products **2** to be obtained in a step- and atom-economical fashion from **1**. In addition, more advanced adducts **5** can be directly synthesized from **2** using established decarboxylative functionalization strategies with photoredox catalysts.⁸

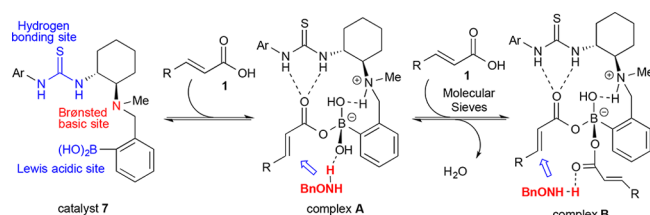
Recently, carboxylates have played an important role in ion-pair catalysis using chiral thioureas.⁹ This concept has been extended to a variety of asymmetric reactions, but carboxylates that form dual hydrogen bonds with thioureas only work as chirality transmitters and have never been used as electrophiles.¹⁰ In contrast, various arylboronic acids have been developed for the direct condensation of carboxylic acids with amines or alcohols.¹¹ Therefore, we envisioned that the synergistic interaction of carboxylate anions with both thiourea and arylboronic acid would enable direct Michael addition to **1**. Accordingly, we have developed the first asymmetric aza-Michael addition^{12a} of *O*-benzylhydroxylamine **6** to α,β -unsaturated carboxylic acid **1a** using catalyst **7a** to afford β -amino acid derivative **2a** (eq 1) and the asymmetric



intramolecular oxa-Michael addition^{12b} of phenolic α,β -unsaturated carboxylic acids using dual catalysts of a chiral bifunctional thiourea^{12c,d} and arylboronic acid. However, no spectroscopic evidence was obtained for the reaction mechanism of the aza-Michael addition. Herein, to improve the enantioselectivity and clarify the reaction mechanism, we investigated the following concepts: (i) how catalyst **7** interacts with substrate **1a** and nucleophile **6** to furnish (*S*)-**2a** as the major enantiomer; (ii) why 4 Å molecular sieves (4 Å MS) were required to promote the reaction; (iii) why, in some cases, the enantioselectivity was significantly influenced by the β -substituents of substrates **1** (68–86% ee); and (iv) can a green solvent be used instead of volatile CCl₄, which was a major disadvantage of this reaction.

In our previous work, we hypothesized that catalyst **7** would form zwitterionic complex **A** with carboxylic acid **1** through the acid–base interaction of **1** with the Brønsted basic moiety of **7** (Scheme 2), in which the resulting carboxylate anion is stabilized by both the thiourea and arylboronic acid moieties of the catalyst. The subsequent 1,4-addition of BnONH₂ to the *s-trans* form of the coordinated carboxylic acid occurred from the top side, assisted by the borate hydroxy group, affording

Scheme 2. Possible Catalyst–Substrate Complexes



(*S*)-**2a** predominantly. However, borate complexes **B** can also be generated from complex **A** by a second ligand exchange with another molecule of substrate **1**. In both complexes **A** and **B**, the thiourea can activate the carbonyl oxygen through dual hydrogen-bonding interactions, thereby promoting nucleophilic addition. To identify which complex is more plausible in terms of the nucleophile activation mode, several spectral analyses and kinetic studies were performed to describe the reaction mechanism of the aza-Michael addition. The origin of enantioselectivity was also examined via DFT calculations.

Furthermore, based on these results, we have rationally designed a new catalyst and identified efficient additives and environmentally friendly solvents to enhance reaction selectivity. Finally, the optimized reactions were successfully applied to the formal asymmetric synthesis of pharmaceutically important molecules sitagliptin and α -tocopherol.

RESULT AND DISCUSSION

To obtain structural information on the catalyst, we first performed X-ray crystallographic analysis. Fortunately, a suitable crystalline solid was obtained by recrystallizing **7b** from acetone–hexane (Figure 1)¹³ As expected,¹⁴ intra-

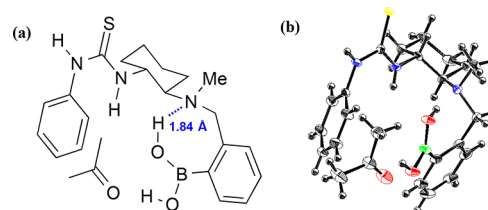


Figure 1. (a) Structure of complex **7b** and acetone in the solid state. (b) ORTEP drawing of **7b**-acetone.

molecular hydrogen bonding was observed between one of the hydroxyl groups of the boronic acid and the tertiary amino group. More importantly, the boronic acid and thiourea face each other, which allows simultaneous activation of the resulting carboxylate anion by both the thiourea and arylboronic acid moieties, particularly with the *syn* arrangement of the thiourea NH groups.¹⁵

We next measured ¹¹B NMR spectra to determine the coordination number of the boron atom of **7b** in solution (Figure 2). The spectrum of **7b** showed a broad single peak at 28 ppm in CDCl₃, indicating that the boron atom exists as a trigonal planar species according to literature values (Figure 2a).¹⁶ This result was in good agreement with the X-ray crystallographic studies above (Figure 1). However, the addition of 4 Å MS to the catalyst solution resulted in the appearance of new signals at 4 and 8 ppm, in addition to the original peak (Figure 2b).

The complexes could not be identified by ¹H NMR analysis, but DOSY NMR experiments indicated the dimerization of catalyst **7b** (see Figure S5 in the Supporting Information). In fact, a signal for dimeric boron complex of **7b** (calcd for C₄₂H₅₅B₂N₆O₃S₂⁺ [M + H]⁺ 777.3958) was observed at 777.3983 in the ESI-MS spectrum (see Figure S7 in the Supporting Information). The dimeric form of the catalyst is thus considered to be generated by releasing 1 equiv of water from two molecules of **7b** in the presence of 4 Å MS (Scheme 3). The signal at 28 ppm in the ¹¹B NMR spectrum can be assigned to the trigonal boron dimer complex, but the two signals at 4 and 8 ppm suggest that tetrahedral borate

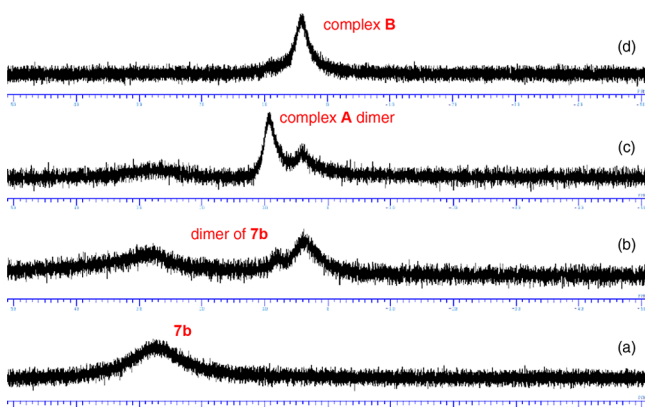
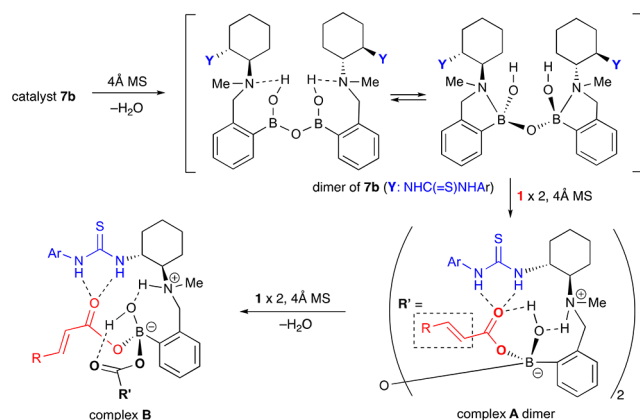


Figure 2. ^{11}B NMR titration experiments of catalyst **7b** with crotonic acid **1b** in CDCl_3 (0.033 M): (a) **7b**; (b) **7b** with 4 Å MS; (c) **7b** with **1b** (1 equiv) and 4 Å MS; (d) **7b** with **1b** (10 equiv) and 4 Å MS.

Scheme 3. Dimerization of **7b** and Complex A in the Presence of 4 Å MS



complexes, for instance, species with coordinated tertiary amino groups, might also be formed. Interestingly, no peak of boroxine of **7b** was detected in the ESI-MS spectrum.

In contrast, when 1 equiv of crotonic acid **1b** was added in the presence of 4 Å MS, the peak at 28 ppm almost disappeared, with a new peak appearing at 9 ppm (Figure 2c), which could be assigned to B–O–B-bridged dimeric forms of complex **A**,¹⁷ as shown in Scheme 3.¹⁸ With a large excess of crotonic acid (**7b** and **1b** in a 1:10 ratio), another new signal at 4 ppm was only observed (Figure 2d). This signal was assigned to complex **B**, which can be readily formed in the reaction of complex **A** dimer with another two molecules of carboxylic acid (Scheme 3 and see Figure S6 in the Supporting Information). Notably, without 4 Å MS, almost no peaks were observed at 4 and 9 ppm, even in the presence of 10 equiv of **1b** (see Figure S3 in the Supporting Information). The presence of 4 Å MS seems to be essential for the generation of the tetrahedral borate complexes, and complex **B** was presumed to play an important role in the enantioselective Michael addition.¹⁹

To confirm whether two carboxy groups could coordinate to the boron atom of **7b**, we performed ^{11}B NMR titration experiments of **7b** with maleic acid **8** (Figure 3). Interestingly, when 0.5 equiv of **8** was added, only two major peaks at 28 and 3 ppm were observed (Figure 3b), which were distinct from the results in Figure 2c. Increasing the ratio of **7b**/**8** to 1:1 and

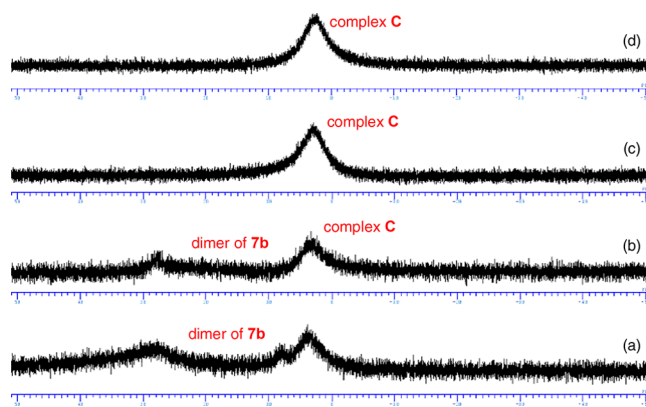


Figure 3. ^{11}B NMR titration experiments of **7b** with maleic acid **8** in CDCl_3 (0.033 M): (a) **7b** with 4 Å MS; (b) **7b** with **8** (0.5 equiv) and 4 Å MS; (c) **7b** with **8** (1.0 equiv) and 4 Å MS; (d) **7b** with **8** (2.0 equiv) and 4 Å MS.

1:2 caused the signal at 28 ppm to disappear, with the same peak at 3 ppm developing (Figure 3c,d). These results suggest that both carboxy groups in **8** could be incorporated into borate complexes, as in complex **C**, shown in Figure 4.

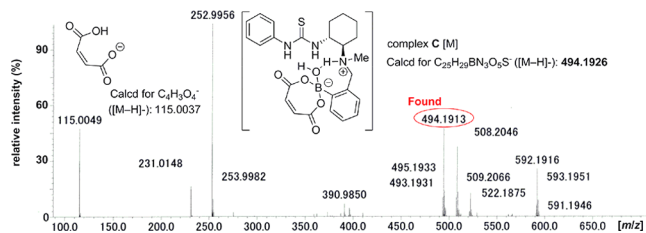


Figure 4. Detection of complex **C** by ESI-MS analysis.

We further performed ESI-MS analyses²⁰ of mixtures of **7b**/**1b** and **7b**/**8** in the presence of 4 Å MS to identify borate complexes **A**–**C**. Despite multiple trials, we could not detect the exact mass signals of complex **A** dimer and double-coordinated complex **B** due to their instability and only observed a signal for monocoordinated complex **A** at 482.2272, irrespective of the **7b**/**1b** ratio (see Figures S8 and S9 in the Supporting Information). In contrast, when catalyst **7b** and maleic acid **8** were mixed in a 1:1 ratio, the exact mass peak of complex **C** (calcd for $\text{C}_{25}\text{H}_{29}\text{BN}_3\text{O}_5\text{S}^-$ $[\text{M} - \text{H}]^-$ 494.1926) was detected as a major peak at 494.1913 with errors of no more than 5 ppm in the negative region of the spectrum. Complex **C** is thought to be generated by the dehydration of complex **A** dimer consisted of **7b** and **8**.

In addition to these spectroscopic analyses, we performed kinetic studies using classical initial rate kinetics for the reaction shown in eq 1. Using an excess of **6**, the reaction rate became greater, as the concentration of **1a** was increased gradually from 5.0 to 20 mM (Figure 5a). The reaction rates vs concentration plot reveals a linear relationship for the initial phase of the reaction (Figure 5b), pointing to first-order kinetics in substrate **1a**. Regarding the nucleophile **6**, the kinetic measurements similarly suggest first-order rate dependence in the initial phase (see Figure 5c,d). Additional kinetic data indicate that the reaction rate is reduced after the initial period (see Figures S10a and S11a). This latter kinetic behavior is likely due to product inhibition, which could be supported by further experiments. Addition of product **2a** to

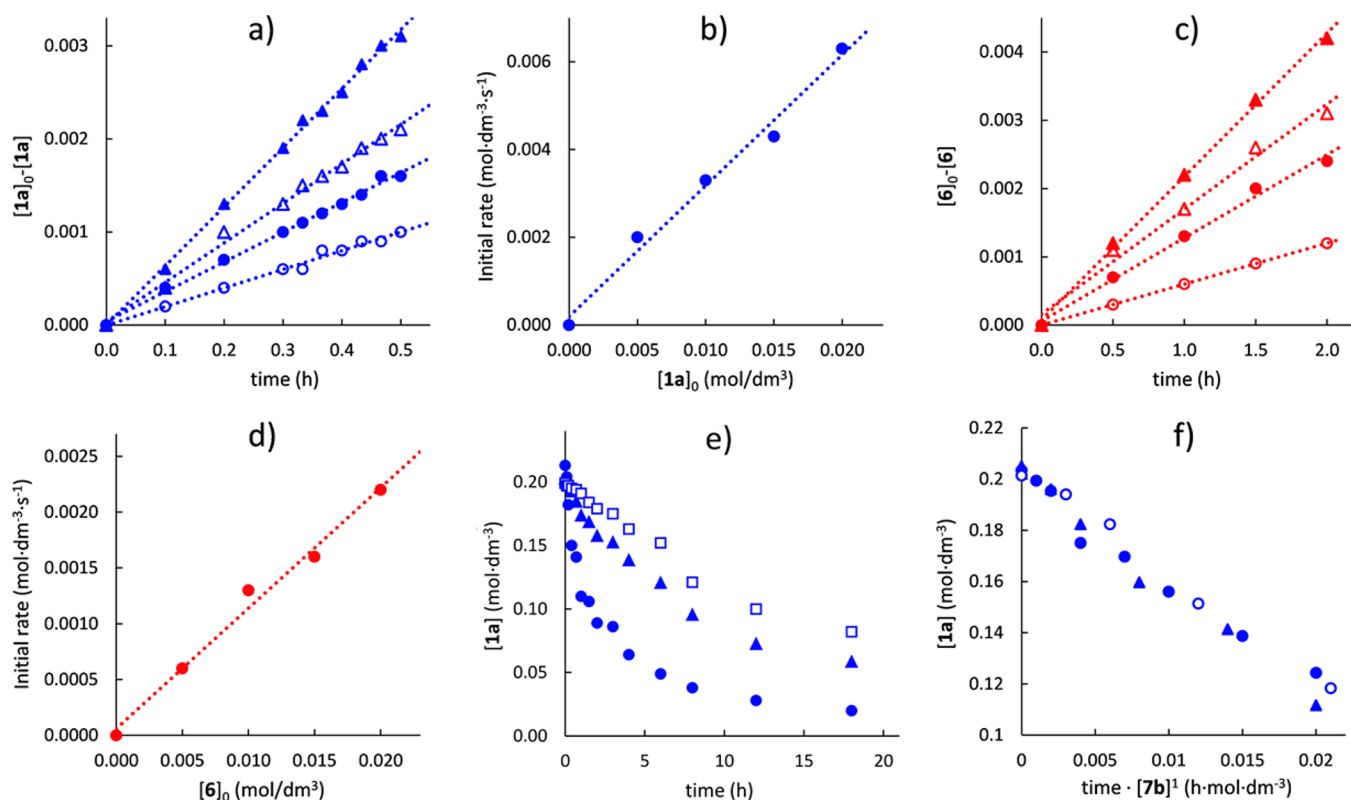
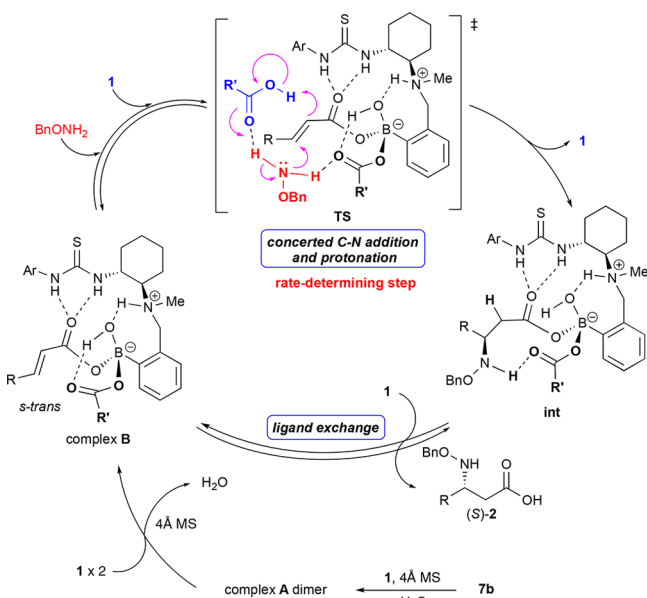


Figure 5. Kinetic studies of the reaction of carboxylic acid **1a** and BnONH_2 **6** catalyzed by **7b** with 4 Å MS in CCl_4 . (a) $([\mathbf{1a}]_0 - [\mathbf{1a}])$ vs time using an excess (10 equiv) of **6** (first 0.5 h) [blue \blacktriangle , 20 mM; blue \triangle , 15 mM; blue \bullet , 10 mM; blue \circ , 5.0 mM of **1a**]. (b) $(d[\mathbf{1a}]/dt)$ vs $[\mathbf{1a}]_0$. (c) $([\mathbf{6}]_0 - [\mathbf{6}])$ vs time using an excess (10 equiv) of **1a** (first 2.0 h). [red \blacktriangle , 20 mM; red \triangle , 15 mM; red \bullet , 10 mM; red \circ , 5.0 mM of **6**]. (d) $(d[\mathbf{6}]/dt)$ vs $[\mathbf{6}]_0$. (e) $[\mathbf{1a}]$ vs time with and without product **2a** [blue \bullet , standard conditions; blue \blacktriangle , with **2a** added at time = 0; blue \square , with **2a** mixed with catalyst **7b** for 4 h prior to reaction]. (f) $[\mathbf{1a}]$ vs $\text{time} \cdot [\mathbf{7b}]^1$ ([blue \bullet , 5 mol %; blue \blacktriangle , 10 mol %; blue \circ , 15 mol % in $[\mathbf{7b}]$]).

the reaction mixture retarded the reaction significantly (Figure 5e).²¹ Finally, the reaction was found to be first order with respect to the catalyst **7b**, as illustrated by the overlay of conversion curves on the $[\mathbf{1a}]$ vs $\text{time} \cdot [\mathbf{7b}]^1$ plot (Figure 5f).²²

A plausible reaction mechanism emerging from the results of NMR titration and kinetic experiments is shown in Scheme 4.

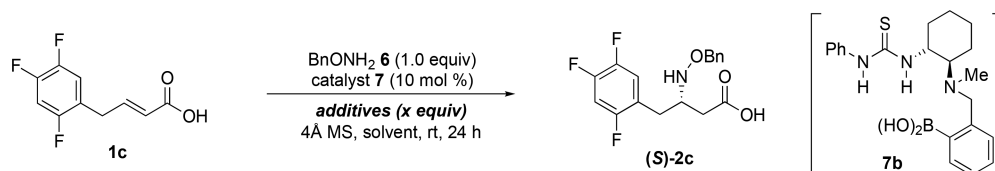
Scheme 4. Plausible Reaction Mechanism



The molecular sieves play a crucial role in the formation of dimeric catalyst, which readily reacts with carboxylic acid **1** to form a dimer of tetracoordinated borate complex **A** and subsequently complex **B**. This latter process is accompanied by the release of water as well. In contrast, the dimerization of neither **7b** nor complex **A** can occur in the absence of 4 Å MS. In complex **B**, one of the coordinated carboxylate ligands is thought to form hydrogen bonds with the thiourea NH groups. The second coordinated carboxylate may act as a Brønsted base that binds and activates the nucleophile via H-bonding interactions. Based on the first-order kinetics in both substrates (**1** and **6**), we anticipate that complex **B** is the resting state of the catalytic cycle in the initial phase of the reaction, and the rate-determining C–N addition step takes place via the assistance of an additional carboxylic acid (see transition state **TS** in Scheme 4). The reaction likely proceeds via proton transfer from the NH_2 group to the sp^2 carbon of the adduct to give intermediate **int**. This species is analogous to complex **B**, but it involves a product carboxylic acid. The catalytic cycle is finally completed by subsequent ligand exchange by substrate **1** to furnish the desired product **2**.

The observed product inhibition implies that the resting state shifts from complex **B** to intermediate **int** as the reaction proceeds. Due to additional noncovalent interactions between the product and the catalyst, the **int** state may indeed be thermodynamically more stable than complex **B**, and therefore, it may become more populated at higher conversions.²³

The proposed mechanism is consistent with the kinetic data and underlines the importance of the second coordinated

Table 1. Effect of Carboxylic Acids as Additives and Reoptimization of Reaction Conditions^a

entry	catalyst	additive (equiv)	solvent	yield ^b (%)	ee ^c (%)
1	7a	none	CCl ₄	84	73
2	7b	none	CCl ₄	77	76
3	7a	none	Cl ₂ C=CCl ₂	47	48
4	7b	none	Cl ₂ C=CCl ₂	73	55
5	7a	none	4-CF ₃ C ₆ H ₄ Cl	31	55
6	7b	none	4-CF ₃ C ₆ H ₄ Cl	57	69
7	7b	PhCO ₂ H (1.0)	CCl ₄	85	97
8	7b	PhCO ₂ H (1.0)	Cl ₂ C=CCl ₂	77	95
9	7b	PhCO ₂ H (1.0)	4-CF ₃ C ₆ H ₄ Cl	53	92
10	7b	AcOH (1.0)	Cl ₂ C=CCl ₂	6	26
11	7b	4-MeOC ₆ H ₄ CO ₂ H (1.0)	Cl ₂ C=CCl ₂	69	88
12	7b	4-CF ₃ C ₆ H ₄ CO ₂ H (1.0)	Cl ₂ C=CCl ₂	67	90
13	7b	2-MeOC ₆ H ₄ CO ₂ H (1.0)	Cl ₂ C=CCl ₂	80	85
14	7b	PhCO ₂ H (0.5)	Cl ₂ C=CCl ₂	77	86
15	7b	PhCO ₂ H (2.0)	Cl ₂ C=CCl ₂	69	94
16	7b	PhCO ₂ H (5.0)	Cl ₂ C=CCl ₂	40	91

^aUnless otherwise noted, the reaction was carried out using **1c** (1.0 mmol), **6** (1.0 equiv), catalyst **7a** or **7b** (0.1 equiv), and 4 Å MS at room temperature for 24 h. ^bIsolated yield after treatment with TMSCHN₂. ^cEstimated by chiral HPLC after treatment with TMSCHN₂.

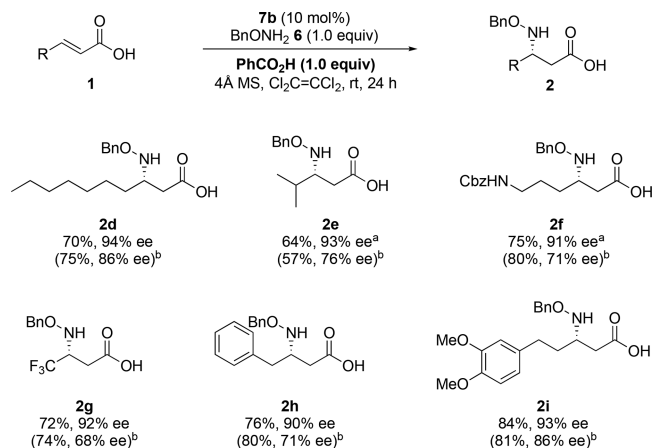
carboxylate unit in the present stereoselective transformation. The revealed mechanism suggests that the addition of different unreactive carboxylic acids, such as benzoic acid, as Brønsted acids/bases might improve the reaction rate and enantioselectivity by altering the 1,4-addition and/or proton-transfer steps.

To test this hypothesis, we investigated the effect of a variety of carboxylic acids as additives and the reoptimization of solvent and catalyst. Using the asymmetric synthesis of sitagliptin, an antidiabetic drug,^{3b,24} as the goal, the reaction of *O*-benzylhydroxylamine **6** with fluorinated carboxylic acid **1c** was screened using a range of carboxylic acid additives in several solvents (Table 1). When the reaction was performed with **7a** or **7b** without any additives in various halogenated solvents (CCl₄, Cl₂C=CCl₂, 4-CF₃C₆H₄Cl), **7b** always gave better enantioselectivities for desired product **2c** than **7a** (entries 1–6). We then examined the effect of additive with **7b** in halogenated solvents. To our delight, adding benzoic acid (1 equiv) significantly enhanced the ee of **2c**, irrespective of the solvent used (entries 7–9). For further screening, tetrachloroethylene was selected as a solvent to examine types and amounts of additives. Electron-rich and electron-poor benzoic acids, and AcOH, did not surpass benzoic acid in terms of enantioselectivity (entries 10–13) but did support the proposed reaction mechanism via complex **B** (Scheme 4), where electron-rich and less bulky additives competed with **1** to form three ternary complexes **B**, such as **7b**·**1**, **7b**·**1**·(additive), and **7b**·(additive)₂, composed of two carboxylates. Consequently, the predominant generation of homodicarboxy borate complex **7b**·(additive)₂ lowered the yield of **2**, and heterodicarboxy borate complex **7b**·**1**·(additive) resulted in either higher or lower ee values for **2**, depending on the additive. Increasing the amount of benzoic acid additive led to a lower yield, for the same reason as described above, together

with a slight improvement in selectivity (entries 14–16), in agreement with the proposed mechanism.

With optimized reaction conditions in hand, we further explored the substrate scope, as shown in Scheme 5. Notably,

Scheme 5. Improved Substrate Scope of Optimized Conditions



^aReaction time was 48 h. ^bThe results with **7a** in the absence of PhCO₂H are indicated in parentheses.

the enantioselectivities of products **2d–i** (90–94% ee) were greatly improved by adding benzoic acid in comparison with the previous outcomes (68–86% ee), while the product yields were not significantly affected.

To gain insight into the origin of enantioselectivity, we carried out DFT calculations for the stereogenic C–N bond formation step of the reaction.²⁵ The particular system we considered involves catalyst **7b**, reactants **1b** and **6**, and benzoic acid as the additive. Based on the results of kinetic

analysis (i.e., first-order kinetic dependence on both acid **1** and nucleophile **6**), we assumed that the C–N addition step is coupled with the protonation process, which occurs via the involvement of an extra carboxylic acid (benzoic acid in the present model).

Transition states corresponding to the addition of nucleophile **6** to ternary complex **7b·1b·(PhCO₂)** (complex **B** in Scheme 4) in the presence of a benzoic acid were explored computationally and the most stable structures leading to (*S*) and (*R*) product enantiomers are depicted in Figure 6. In

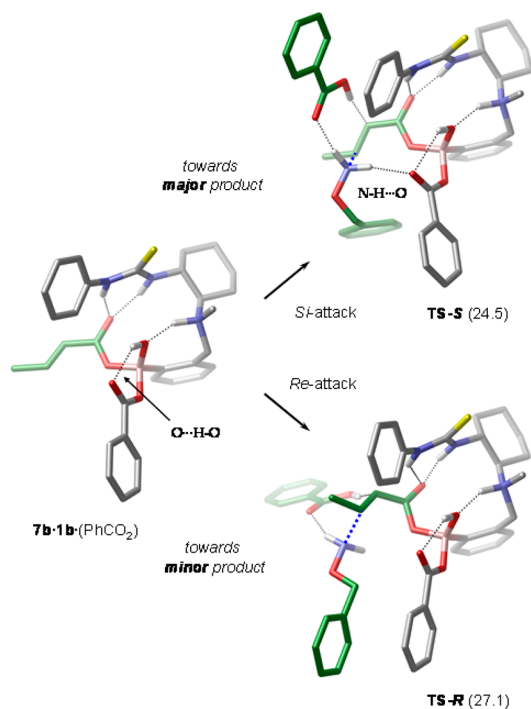


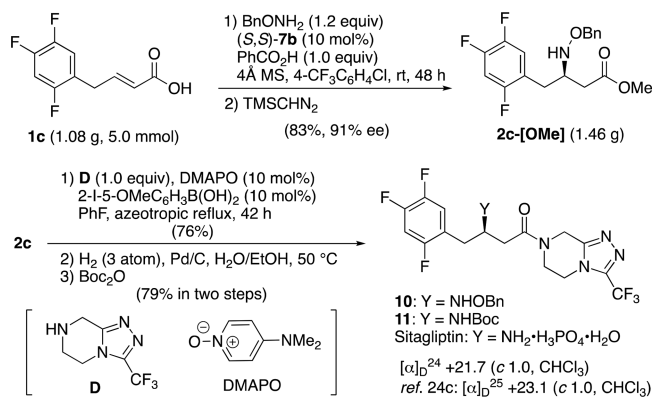
Figure 6. Acid-assisted C–N bond formation transition states leading to (*S*) and (*R*) product enantiomers in the aza-Michael reaction of **6** and **1b**. Relative stabilities are given in kcal/mol with respect to **7b·1b·(PhCO₂)** + **6** + PhCO₂H. The H-bonding interactions are indicated as dotted lines. The developing C–N bond is shown as a blue dotted line. All C–H hydrogen atoms are omitted for clarity. The C atoms of the reacting partners are highlighted in green.

intermediate **7b·1b·(PhCO₂)**, the electrophile is attached to the catalyst via a covalent B–O bond and its orientation is fixed by a double H-bond formed with the thiourea. The benzoyloxy ligand is anchored via an intramolecular O–H...O bond, such that the oxygen atom that activates the nucleophile is positioned above the *Si* face of the crotonate double bond. This structural arrangement in **7b·1b·(PhCO₂)** enables nucleophile activation (via N–H...O(benzoate) H-bonding interaction) only for *Si*-face attack of the crotonate (see **TS-S** in Figure 6). In this transition state, the benzoic acid is bound to the second NH group of the nucleophile via the carbonyl moiety, whereas the acidic OH group is oriented toward the proton acceptor carbon atom of the crotonate. The calculations reveal that the C–N addition and the proton-transfer processes are indeed coupled, as transition state **TS-S** represents a concerted asynchronous mechanism, wherein the acid-assisted C–N addition occurs first followed by a double proton transfer event (concerted protonation of the substrate by the acid OH and deprotonation of the NH₂ group by the acid carbonyl).²⁶ An analogous transition state was identified

computationally for the *Re*-face attack of the crotonate as well; however, in that transition state (**TS-R** in Figure 6), the nucleophile is not activated due to the lack of N–H...O(benzoate) interaction. The revealed mechanism, which identifies the irreversible C–N addition/protonation event as the enantioselectivity-determining step, is in accordance with the kinetic data and also accounts well for the observed enantioselectivity (the barriers calculated for the C–N bond formation step for the *Si* and *Re* pathways are 24.5 and 27.1 kcal/mol, respectively).

To demonstrate the applicability of the established aza-Michael addition, the asymmetric synthesis of sitagliptin was carried out on a gram scale (Scheme 6). In this case, 4-

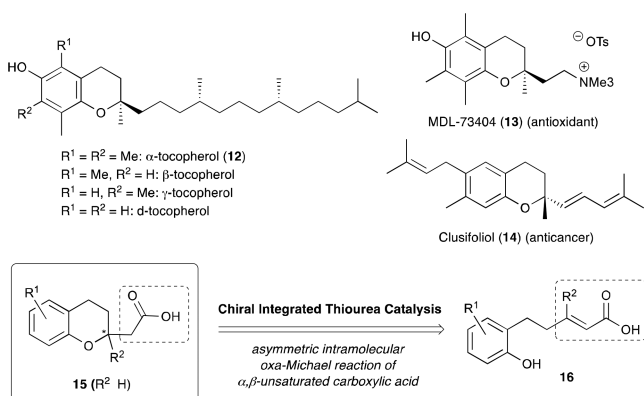
Scheme 6. Synthetic Application to Sitagliptin



CF₃C₆H₄Cl (PCBTf), which has been used in chemical manufacturing due to its high boiling point and recyclability, was adopted as the solvent instead of CCl₄ and Cl₂C=CCl₂. The reaction of **1c** (1.08 g) with BnONH₂ (1.2 equiv) in the presence of (*S,S*)-**7b**, an enantiomer of **7b**, gave the desired ester **2c**-[OMe] (1.46 g) in two steps without suffering from a decrease in enantioselectivity (91% ee). Following the procedure developed by Ishihara,¹¹⁰ the obtained adduct **2c** was converted into corresponding amide **10** by catalytic amidation with bicyclic amine **D** without using conventional condensing reagents. Successive subsection of amine **10** to Pd/C-mediated hydrogenolysis and Boc-protection furnished the known *N*-Boc derivative of sitagliptin in good yield. The synthetic compound was identical to an authentic sample by a comparison of spectral data.^{24c}

Having clarified the mechanism of asymmetric aza-Michael addition and having optimized the reaction conditions in terms of additive and solvent, we next attempted to synthesize optically active chroman derivatives, which are common in natural products and biologically active compounds (Scheme 7). Among these, chromans bearing tetrasubstituted chiral carbon centers, such as tocopherols,²⁷ MDL-73404,²⁸ and clusifoliol,²⁹ have attracted much attention from synthetic chemists due to their unique structure and biological activities. Indeed, several elegant asymmetric syntheses toward α -tocopherol have been reported using intramolecular *O*-alkylation,³⁰ oxidative C–O bond formation,³¹ and an oxa-Michael addition.^{4e,32} However, constructing the chroman scaffold while incorporating the tetrasubstituted carbon center in a stereocontrolled manner remains challenging.³³ In particular, there have been no successful examples of asymmetric oxa-Michael addition to β,β -disubstituted- α,β -unsaturated carboxylic acid surrogates due to the weak

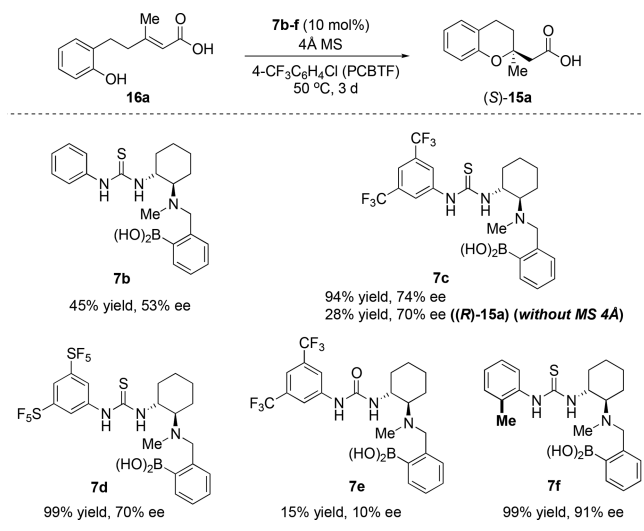
Scheme 7. Strategy for the Construction of Chroman Scaffolds with Chiral Tetrasubstituted Carbon Centers



nucleophilicity of the oxygen nucleophile and the low reactivity of the Michael acceptor. We envisioned that our catalysts **7** would recognize the carboxylic acid and phenolic OH of substrate **16** through the thiourea and arylboronic acid, as in complex **B** in Scheme 4, to facilitate stereoselective transformation into desired product **15**.

Based on this hypothesis, we first investigated the reaction of α,β -unsaturated carboxylic acid **16a** as a model substrate (Scheme 8). In fact, the reaction of **16a** under dual catalytic

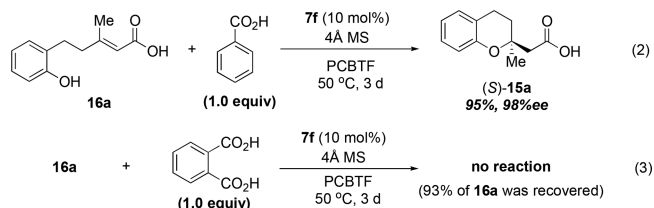
Scheme 8. Optimization of Reaction Conditions



conditions previously reported by our group^{12b} gave desired product **15a**, albeit with a low yield and ee. However, when 10 mol % of **7b** was used in PCBTF at 50 °C, the reaction proceeded slowly to afford the desired product in 45% yield with 50% ee after 3 days. To our delight, catalysts **7c** and **7d**, bearing electron-withdrawing groups CF_3 and SF_5 , respectively, on the aromatic ring, improved both the yields (94–99%) and enantioselectivities (70–74% ee), while the corresponding urea catalyst **7e**, bearing 3,5- CF_3 substituents, resulted in a lower yield and selectivity. Notably, 4 Å MS were again important for achieving high enantioselectivities for the tetrasubstituted chiral carbon center in product **15**. For instance, when the reaction of **16a** was performed without 4 Å MS in the presence of 10 mol % of **7c**, the opposite enantiomer, $(R)\text{-}15a$, was obtained with 70% ee, albeit in a low yield (28% yield after 3 days). We further explored the effect of

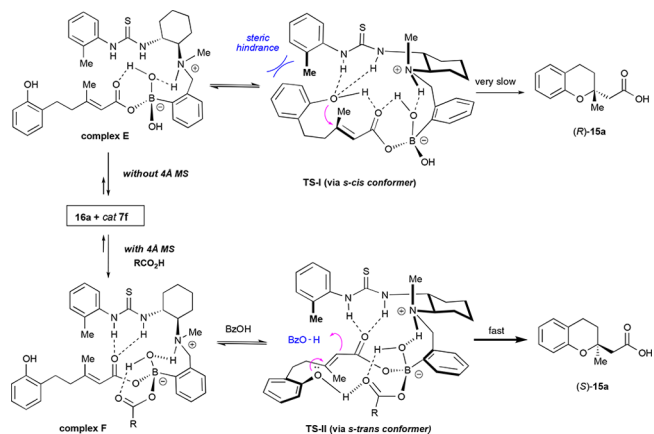
aryl substituent in the catalysts on the enantioselectivity to suppress the undesired pathway to the (R) -isomer. Of these, catalyst **7f**, which possessed an *o*-methyl group on the aromatic ring, afforded the best results (99% yield, 91% ee). However, our additional experiments demonstrated that there is no strong correlation between the reaction rate (or yield) and the electron density of aryl groups. We suspect that the solubility of these catalysts in PCBTF is important for good yields, while a rational explanation of these results is still needed (see page S17 in the Supporting Information).

Similar to the aza-Michael addition, the enantioselectivity was further improved to 98% ee when 1 equiv of benzoic acid was added to the reaction mixture (eq 2). In contrast, the



addition of *o*-phthalic acid (1.0 equiv) completely shut down the reaction, affording no desired product (eq 3). Double-coordination of the carboxylate to the boron center of **7f** seemed to play a crucial role in the enantioselectivity, as seen for the intermolecular aza-Michael addition. These results strongly suggested that our catalytic system using ternary borate complexes would be generally applicable to a range of asymmetric reactions.

Taking all of the results into account, we proposed a plausible reaction mechanism, as shown in Scheme 9. Substrate

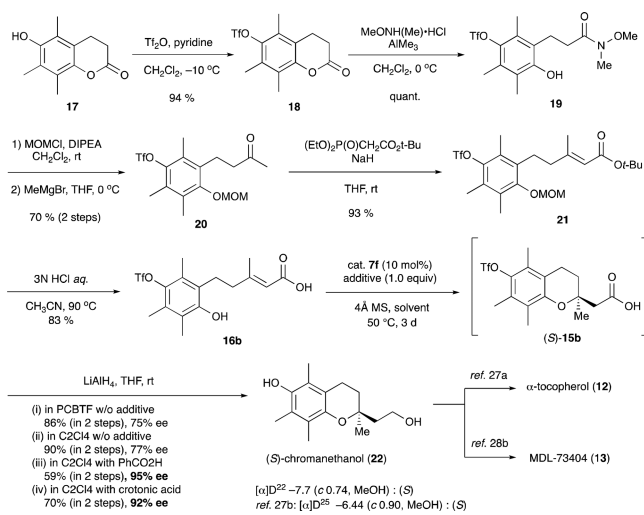
Scheme 9. Possible Mechanism Explaining the Effect of 4 Å MS and the *o*-Me Group in Catalyst **7f**

16a and catalyst **7f** form complex **E** via acid–base interactions, where the linear *s*-cis conformer would be favorable. In the presence of molecular sieves, another carboxylic acid (substrate or additive) coordinates to the borate complex as a second ligand to give complex **F**. Although **TS-II**, adopting the *s*-trans conformer, seems unfavorable compared to *s*-cis **TS-I**, the interaction of the second carboxylate with the phenolic OH group in **16a** makes the 1,4-addition via **TS-II** relatively fast, furnishing product $(S)\text{-}15a$, whose absolute configuration is in good agreement with the experimental results. In this case, the oxa-Michael addition and protonation probably takes place in a stepwise manner because of the bulkiness of the 2-tolyl group

of **7f**. Even in the absence of molecular sieves, the reaction proceeds via **TS-I**, where intramolecular hydrogen bonding between the phenolic OH and carbonyl group of the substrate promotes the Michael addition from the *Re* face without participation of the borate carboxylate. However, distinct from the cyclization via **TS-II**, the reaction occurs very slowly because reactive complex **F** is not sufficiently produced in the absence of 4 Å MS. Moreover, the effect of the *o*-methyl substituent in catalyst **7f** can be neatly explained by its repulsion of the phenol ring in the substrate in **TS-I**, affording (*S*)-**15a** in higher ee through the predominant reaction via **TS-II**.

Finally, the established oxa-Michael addition was applied to the formal asymmetric synthesis of tocopherol (**Scheme 10**).

Scheme 10. Asymmetric Synthesis of Key Intermediate **22** toward Chroman Derivatives



Starting from known lactone **17**,³⁴ Weinreb amide **19** was synthesized via sulfonamide **18** by successive treatment of **17** with TiF_2O and $\text{MeONHMe}/\text{AlMe}_3$. After **19** was converted to its corresponding MOM ether, the obtained product was subjected to methylation with MeMgBr to afford ketone **20**, which was then transformed into α,β -unsaturated carboxylic acid (*E*)-**16b** in 72% yield using the Horner–Wadsworth–Emmons reaction and acid hydrolysis. As expected, the key intramolecular oxa-Michael reaction of **16b** took place in an enantioselective manner, giving cyclized adduct **15b** in good yield. However, the product could not be isolated in a pure form due to contamination of the additive. Oxa-Michael adduct **15b** was converted into known compound **22** by treatment with LiAlH_4 via reduction of the carboxy group together with deprotection of the triflate group. Compound **22** had moderate to high ee values depending on the solvent and additive, as shown in **Scheme 10**. Under the best conditions (1.0 equiv of crotonic acid additive in $\text{Cl}_2\text{C}=\text{CCl}_2$ at 50 °C), target compound **22** was obtained in 70% yield (over two steps) with 92% ee. The absolute configuration of **22** was determined to be *S* by comparing its specific optical rotation value with the literature value.^{27b} As obtained chromanethanol **22** has been successfully transformed into α -tocopherol^{27a} and MDL-73404,^{28b} we achieved a concise formal asymmetric synthesis of these molecules in only eight steps involving the asymmetric oxa-Michael addition using our original thiourea catalysts.

CONCLUSION

We have developed multifunctional chiral thiourea catalysts composed of a tertiary amine and arylboronic acid. These hybrid catalysts (**7**) can form 1:2 complexes containing 2 equiv of homo- or heterocarboxylic acids, which concurrently activate the carboxy group of the coordinated substrate and heteroatoms of nucleophiles through multiple hydrogen bonding interactions, in a manner similar to that for enzymes. The resulting ternary complexes accelerate asymmetric intermolecular aza-Michael addition of *N*-benzylhydroxylamine and asymmetric intramolecular oxa-Michael addition of phenol. The products of both reactions can be efficiently applied to the asymmetric synthesis of pharmaceutically important molecules on either a gram scale or via short-step routes. Spectral data and kinetic studies showed that molecular sieves play a critical role in the double coordination of carboxylic acids to catalysts, leading to the formation of catalytically active ternary borate complexes. These ternary borate complexes, comprising thiourea, arylboronic acid, and carboxylates, function as both Brønsted and Lewis acids, and Brønsted base, which could be supported by computations. We think that this concept will help to develop a novel catalytic system for the selective activation of carboxylic acids, for which research is now underway in our laboratory.

ASSOCIATED CONTENT

Supporting Information

The Supporting Information is available free of charge on the ACS Publications website at DOI: 10.1021/jacs.8b07511.

X-ray data for compound **7b** (CIF)

Mechanistic studies using DFT calculations (PDF)

Experimental procedures, characterization data, ¹¹B NMR studies, ESI-mass spectra, kinetic studies, ¹H, ¹³C NMR spectra, and HPLC analyses (PDF)

AUTHOR INFORMATION

Corresponding Authors

*papai.imre@ttk.mta.hu

*takemoto@pharm.kyoto-u.ac.jp

ORCID

Yusuke Kobayashi: 0000-0003-3074-7378

Imre Pápai: 0000-0002-4978-0365

Yoshiji Takemoto: 0000-0003-1375-3821

Notes

The authors declare no competing financial interest.

ACKNOWLEDGMENTS

This work was supported by JSPS KAKENHI Grant No. 16H06384 and by the Hungarian Scientific Research Fund (OTKA, Grant No. K-112028). Computer facilities provided by NIIF HPC Hungary (Project 85708 kataproc) are also acknowledged.

REFERENCES

- (1) For a review, see: (a) Hoffmann, R. W. *Synthesis* **2006**, 2006, 3531–3541. (b) Young, I. S.; Baran, P. S. *Nat. Chem.* **2009**, 1, 193–205. (c) Gaich, T.; Baran, P. S. *J. Org. Chem.* **2010**, 75, 4657–4673. (d) Saicic, R. N. *Tetrahedron* **2014**, 70, 8183–8218.
- (2) For reviews, see: (a) Monge, D.; Jiang, H.; Alvarez-Casao, Y. *Chem. - Eur. J.* **2015**, 21, 4494–4504. (b) Desimoni, G.; Faita, G.; Quadrelli, P. *Chem. Rev.* **2015**, 115, 9922–9980. For selected

examples of catalytic asymmetric conjugate addition of activated α,β -unsaturated carboxylic acid derivatives, see: (c) Gandelman, M.; Jacobsen, E. N. *Angew. Chem., Int. Ed.* **2005**, *44*, 2393–2397. (d) Yamagiwa, N.; Qin, H.; Matsunaga, S.; Shibasaki, M. *J. Am. Chem. Soc.* **2005**, *127*, 13419–13427. (e) Inokuma, T.; Hoashi, Y.; Takemoto, Y. *J. Am. Chem. Soc.* **2006**, *128*, 9413–9419. (f) Sibi, M. P.; Itoh, K. *J. Am. Chem. Soc.* **2007**, *129*, 8064–8065. (g) Vakulya, B.; Varga, S.; Soós, T. *J. Org. Chem.* **2008**, *73*, 3475–3480. (h) Didier, D.; Meddour, A.; Bezzene-Lafollée, S.; Collin, J. *Eur. J. Org. Chem.* **2011**, *2011*, 2678–2684. (i) Dai, L.; Yang, H.; Niu, J.; Chen, F.-E. *Synlett* **2012**, *2012*, 314–316. (j) Zhao, B.-L.; Du, D.-M. *Org. Biomol. Chem.* **2014**, *12*, 1585–1594. (k) Fukata, Y.; Asano, K.; Matsubara, S. *J. Am. Chem. Soc.* **2015**, *137*, 5320–5323. (l) Zhang, M.; Kumagai, N.; Shibasaki, M. *Chem. - Eur. J.* **2016**, *22*, 5525–5529. (m) Zhng, Y.; Yao, Y.; Ye, L.; Shi, Z.; Li, X.; Zhao, Z.; Li, X. *Tetrahedron* **2016**, *72*, 973–978.

(3) For selected examples of β -amino acid derivatives, see: (a) Hamada, M.; Tadeuchi, T.; Kondo, S.; Ikeda, Y.; Naganawa, H.; Maeda, K.; Okami, Y.; Umezawa, H. *J. Antibiot.* **1970**, *23*, 170–171. (b) Kim, D.; Wang, L.; Beconi, M.; Eiermann, G. J.; Fisher, M. H.; He, H.; Hickey, G. J.; Kowalchick, J. E.; Leitung, B.; Lyons, K.; Marsilio, F.; McCann, M. E.; Patel, R. A.; Petrov, A.; Scapin, G.; Patel, S. B.; Roy, R. S.; Wu, J. K.; Wyvratt, M. J.; Zhang, B. B.; Zhu, L.; Thornberry, N. A.; Weber, A. E. *J. Med. Chem.* **2005**, *48*, 141–151. For a review of chroman derivatives, see: (c) Shen, H. C. *Tetrahedron* **2009**, *65*, 3931–3952.

(4) For examples of catalytic asymmetric aza-Michael addition of α,β -unsaturated esters, see: (a) Weiß, M.; Borchert, S.; Rémond, E.; Jugé, S.; Gröger, H. *Heteroat. Chem.* **2012**, *23*, 202–209. For examples of catalytic asymmetric intramolecular aza-Michael addition of α,β -unsaturated esters, see: (b) Bandini, M.; Eichholzer, A.; Tragmi, M.; Umani-Ronchi, A. *Angew. Chem., Int. Ed.* **2008**, *47*, 3238–3241. (c) Bandini, M.; Bottoni, A.; Eichholzer, A.; Miscione, G. P.; Stenta, M. *Chem. - Eur. J.* **2010**, *16*, 12462–12473. For an example of catalytic aza-Michael addition of α,β -unsaturated carboxylic acid, see: (d) Angelini, T.; Bonollo, S.; Lanari, D.; Pizzo, F.; Vaccaro, L. *Org. Lett.* **2012**, *14*, 4610–4613. For examples of catalytic asymmetric intramolecular oxa-Michael addition of α,β -unsaturated esters and amides, see: (e) Saito, N.; Ryoda, A.; Nakanishi, W.; Kumamoto, T.; Ishikawa, T. *Eur. J. Org. Chem.* **2008**, *2008*, 2759–2766. (f) Gioia, C.; Fini, F.; Mazzanti, A.; Bernardi, L.; Ricci, A. *J. Am. Chem. Soc.* **2009**, *131*, 9614–9615. (g) Hintermann, L.; Ackerstaff, J.; Boeck, F. *Chem. - Eur. J.* **2013**, *19*, 2311–2321. (h) Kobayashi, Y.; Taniguchi, Y.; Hayama, N.; Inokuma, T.; Takemoto, Y. *Angew. Chem., Int. Ed.* **2013**, *52*, 11114–11118. For examples of catalytic asymmetric sulfa-Michael addition of α,β -unsaturated esters, see: (i) Farley, A. J. M.; Sandford, C.; Dixon, D. J. *J. Am. Chem. Soc.* **2015**, *137*, 15992–15995. (j) Yang, J.; Farley, A. J. M.; Dixon, D. J. *Chem. Sci.* **2017**, *8*, 606–610.

(5) For a review, see: (a) Vellalath, S.; Romo, D. *Angew. Chem., Int. Ed.* **2016**, *55*, 13934–13943. For a recent example, see: (b) Robinson, E. R. T.; Walden, D. M.; Fallan, C.; Greenhalgh, M. D.; Cheong, P. H.-Y.; Smith, A. D. *Chem. Sci.* **2016**, *7*, 6919–6927.

(6) (a) Wu, B.; Szymański, W.; Wybenga, G. G.; Heberling, M. M.; Bartsch, S.; de Wildeman, S.; Poelarends, G. J.; Feringa, B. L.; Dijkstra, B. W.; Janssen, D. B. *Angew. Chem., Int. Ed.* **2012**, *51*, 482–486. (b) Weise, N. J.; Parmeggiani, F.; Ahmed, S. T.; Turner, N. J. *J. Am. Chem. Soc.* **2015**, *137*, 12977–12983.

(7) For selected recent reviews of β -amino acid derivatives, see: (a) March, T. L.; Johnston, M. R.; Duggan, P. J.; Gardiner, J. *Chem. Biodiversity* **2012**, *9*, 2410–2441. (b) Kudo, F.; Miyana, A.; Eguchi, T. *Nat. Prod. Rep.* **2014**, *31*, 1056–1073.

(8) For reviews, see: (a) Xuan, J.; Zhang, Z.-G.; Xiao, W.-J. *Angew. Chem., Int. Ed.* **2015**, *54*, 15632–15641. (b) Liu, P.; Zhang, G.; Sun, P. *Org. Biomol. Chem.* **2016**, *14*, 10763–10777. (c) Le Vaillant, F.; Wodrich, M. D.; Waser, J. *Chem. Sci.* **2017**, *8*, 1790–1800. (d) Roslin, S.; Odell, L. R. *Eur. J. Org. Chem.* **2017**, *2017*, 1993–2007. For selected recent examples, see: (e) Zuo, Z.; Ahneman, D. T.; Chu, L.; Terrett, J. A.; Doyle, A. G.; MacMillan, D. W. C. *Science* **2014**, *345*, 437–440. (f) Griffin, J. D.; Zeller, M. A.; Nicewicz, D. A. *J. Am. Chem.*

Soc. **2015**, *137*, 11340–11348. (g) Tan, X.; Song, T.; Wang, Z.; Chen, H.; Cui, L.; Li, C. *Org. Lett.* **2017**, *19*, 1634–1637.

(9) For reviews of anion binding, see: (a) Brak, K.; Jacobsen, E. N. *Angew. Chem., Int. Ed.* **2013**, *52*, 534–561. (b) Seidel, D. *Synlett* **2014**, *25*, 783–794. For recent examples, see: (c) Lalonde, M. P.; McGowan, M. A.; Rajapaksa, N. S.; Jacobsen, E. N. *J. Am. Chem. Soc.* **2013**, *135*, 1891–1894. (d) Witten, M. R.; Jacobsen, E. N. *Angew. Chem., Int. Ed.* **2014**, *53*, 5912–5916. (e) Mittal, N.; Lippert, K. M.; De, C. K.; Klauber, E. G.; Emge, T. J.; Schreiner, P. R.; Seidel, D. *J. Am. Chem. Soc.* **2015**, *137*, 5748–5758.

(10) For synthetic examples of carboxylate anions as nucleophiles, see: Monaco, M. R.; Fazzi, D.; Tsuji, N.; Leutzsch, M.; Liao, S.; Thiel, W.; List, B. *J. Am. Chem. Soc.* **2016**, *138*, 14740–14749 and references cited therein.

(11) For selected reviews, see: (a) Georgiou, I.; Ilyashenko, G.; Whiting, A. *Acc. Chem. Res.* **2009**, *42*, 756–768. (b) Ishihara, K. *Tetrahedron* **2009**, *65*, 1085–1109. (c) Charville, H.; Jackson, D.; Hodges, G.; Whiting, A. *Chem. Commun.* **2010**, *46*, 1813–1823. (d) Dimitrijević, E.; Taylor, M. S. *ACS Catal.* **2013**, *3*, 945–962. (e) Zheng, H.; Hall, D. G. *Aldrichimica Acta* **2014**, *47*, 41–51. (f) Lundberg, H.; Tinnis, F.; Selander, N.; Adolfsen, H. *Chem. Soc. Rev.* **2014**, *43*, 2714–2742. For recent examples, see: (g) Sakakura, A.; Ohkubo, T.; Yamashita, R.; Akakura, M.; Ishihara, K. *Org. Lett.* **2011**, *13*, 892–895. (h) Gernigon, N.; Al-Zoubi, R. M.; Hall, D. G. *J. Org. Chem.* **2012**, *77*, 8386–8400. (i) Gernigon, N.; Zheng, H.; Hall, D. G. *Tetrahedron Lett.* **2013**, *54*, 4475–4478. (j) Liu, S.; Yang, Y.; Liu, X.; Ferdousi, F. K.; Batsanov, A. S.; Whiting, A. *Eur. J. Org. Chem.* **2013**, *2013*, 5692–5700. (k) Morita, Y.; Yamamoto, T.; Nagai, H.; Shimizu, Y.; Kanai, M. *J. Am. Chem. Soc.* **2015**, *137*, 7075–7078. (l) Mohy El Dine, T.; Erb, W.; Berhault, Y.; Rouden, J.; Blanchet, J. *J. Org. Chem.* **2015**, *80*, 4532–4544. (m) El Dine, T. M.; Rouden, J.; Blanchet, J. *Chem. Commun.* **2015**, *51*, 16084–16087. (n) Tam, E. K. W.; Rita; Liu, L. Y.; Chen, A. *Eur. J. Org. Chem.* **2015**, *2015*, 1100–1107. (o) Ishihara, K.; Lu, Y. *Chem. Sci.* **2016**, *7*, 1276–1280.

(12) (a) Hayama, N.; Azuma, T.; Kobayashi, Y.; Takemoto, Y. *Chem. Pharm. Bull.* **2016**, *64*, 704–717. (b) Azuma, T.; Murata, A.; Kobayashi, Y.; Inokuma, T.; Takemoto, Y. *Org. Lett.* **2014**, *16*, 4256–4259. (c) Okino, T.; Hoashi, Y.; Furukawa, T.; Xu, X.; Takemoto, Y. *J. Am. Chem. Soc.* **2005**, *127*, 119–125. (d) Takemoto, Y. *Chem. Pharm. Bull.* **2010**, *58*, 593–601.

(13) CCDC 1432823 (7b) contains the supplementary crystallographic data for this paper. These data can be obtained free of charge from the Cambridge Crystallographic Data Centre via www.ccdc.cam.ac.uk/data_request/cif.

(14) Coghlan, S. W.; Giles, R. L.; Howard, J. A. K.; Patrick, L. G. F.; Probert, M. R.; Smith, G. E.; Whiting, A. *J. Organomet. Chem.* **2005**, *690*, 4784–4793.

(15) DFT calculations indicate that the *anti* and *syn* conformers of 7b lie reasonably close in free energy and they can easily interconvert in solution (for details, see the [Supporting Information](#)).

(16) (a) Zhu, L.; Shabbir, S. H.; Gray, M.; Lynch, V. M.; Sorey, S.; Anslyn, E. V. *J. Am. Chem. Soc.* **2006**, *128*, 1222–1232. (b) Collins, B. E.; Sorey, S.; Hargrove, A. E.; Shabbir, S. H.; Lynch, V. M.; Anslyn, E. V. *J. Org. Chem.* **2009**, *74*, 4055–4060. (c) Chapin, B. M.; Metola, P.; Lynch, V. M.; Stanton, J. F.; James, T. D.; Anslyn, E. V. *J. Org. Chem.* **2016**, *81*, 8319–8330.

(17) Different dimeric ate complexes [Ar(RCOO)B–O–B(CCOR)Ar] prepared from arylboronic acid and carboxylic acid have been reported: Arkhipenko, S.; Sabatini, M. T.; Batsanov, A. S.; Karaluka, V.; Sheppard, T. D.; Rzepa, H. S.; Whiting, A. *Chem. Sci.* **2018**, *9*, 1058–1072.

(18) The formation of the complex A dimer in the reaction between catalytic dimer and crotonic acid is predicted to be thermodynamically feasible. For a computational analysis on B–O–B-bridged dimeric species, see [Supporting Information](#).

(19) (a) Yamashita, R.; Sakakura, A.; Ishihara, K. *Org. Lett.* **2013**, *15*, 3654–3657. (b) Dimakos, V.; Singh, T.; Taylor, M. S. *Org. Biomol. Chem.* **2016**, *14*, 6703–6711. (c) Mohy El Dine, T.; Evans, D.; Rouden, J.; Blanchet, J. *Chem. - Eur. J.* **2016**, *22*, 5894–5898.

(20) Wang, L.; Dai, C.; Burroughs, S. K.; Wang, S. L.; Wang, B. *Chem. - Eur. J.* **2013**, *19*, 7587–7594.

(21) Premixing product **2a** with catalyst **7b** prior to the addition of substrate **1a** and nucleophile **6** resulted in an even more enhanced inhibition, which further supports the role of complex **B**-type intermediates in the catalytic cycle (for additional comments, see Figure S13 in the [Supporting Information](#)).

(22) For the normalized time scale method applied herein to determine the order in catalyst **7b**, see: Burés, J. *Angew. Chem., Int. Ed.* **2016**, *55*, 2028–2031.

(23) Additional stabilizing noncovalent interactions in **int** can be clearly identified computationally (for details, see the [Supporting Information](#)).

(24) (a) Hansen, K. B.; Balsells, J.; Dreher, S.; Hsiao, Y.; Kubryk, M.; Palucki, M.; Rivera, N.; Steinhuebel, D.; Armstrong, J. D., III; Askin, D.; Grabowski, E. J. *J. Org. Process Res. Dev.* **2005**, *9*, 634–639. (b) Savile, C. K.; Janey, J. M.; Mundorff, E. C.; Moore, J. C.; Tam, S.; Jarvis, W. R.; Colbeck, J. C.; Krebber, A.; Fleitz, F. J.; Brands, J.; Devine, P. N.; Huisman, G. W.; Hughes, G. J. *Science* **2010**, *329*, 305–309. (c) Zhou, S.; Wang, J.; Chen, X.; Aceña, J. L.; Soloshonok, V. A.; Liu, H. *Angew. Chem., Int. Ed.* **2014**, *53*, 7883–7886. (d) Davies, S. G.; Fletcher, A. M.; Thomson, J. E. *Tetrahedron: Asymmetry* **2015**, *26*, 1109–1116. (e) Bae, H. Y.; Kim, M. J.; Sim, J. H.; Song, C. E. *Angew. Chem., Int. Ed.* **2016**, *55*, 10825–10829.

(25) The DFT calculations (geometry optimizations, vibrational analysis, estimation of solvent effects) were carried out at the ω B97X-D/6-311G(d,p) level of theory, but additional single-point energy calculations were performed for each located structure using the larger 6-311++G(3df,3pd) basis set. The reported energetics refers to relative solution-phase Gibbs free energies (with CCl_4 as a solvent). For further details, see the [Supporting Information](#).

(26) It should be noted that the stepwise reaction mechanism of the C–N addition/protonation sequence (with protonation as the rate-determining step) cannot be fully excluded either, but our computations indicate that this scenario is less feasible than the concerted pathway (for related analysis, see [Supporting Information](#)).

(27) (a) Cohen, N.; Eichel, W. F.; Lopresti, R. J.; Neukom, C.; Saucy, G. *J. Org. Chem.* **1976**, *41*, 3505–3511. (b) Grisar, J. M.; Marciniak, G.; Bolkenius, F. N.; Verne-Mismer, J.; Wagner, E. R. *J. Med. Chem.* **1995**, *38*, 2880–2886. (c) Netscher, T. *Vitam. Horm.* **2007**, *76*, 155–202.

(28) (a) Grisar, J. M.; Petty, M. A.; Bolkenius, F. N.; Dow, J.; Wagner, J.; Wagner, E. R.; Haegele, K. D.; De Jong, W. *J. Med. Chem.* **1991**, *34*, 257–260. (b) Mizuguchi, E.; Suzuki, T.; Achiwa, K. *Synlett* **1994**, *1994*, 929–930.

(29) Tanaka, T.; Asai, F.; Iinuma, M. *Phytochemistry* **1998**, *49*, 229–232.

(30) (a) Trost, B. M.; Shen, H. C.; Dong, L.; Surivet, J.-P.; Sylvain, C. *J. Am. Chem. Soc.* **2004**, *126*, 11966–11983. (b) Tietze, L. F.; Sommer, K. M.; Zinngrebe, J.; Stecker, F. *Angew. Chem., Int. Ed.* **2005**, *44*, 257–259. (c) Rein, C.; Demel, P.; Outten, R. A.; Netscher, T.; Breit, B. *Angew. Chem., Int. Ed.* **2007**, *46*, 8670–8673. (d) Tanaka, S.; Seki, T.; Kitamura, M. *Angew. Chem., Int. Ed.* **2009**, *48*, 8948–8951. (e) Uria, U.; Vila, C.; Lin, M.-Y.; Rueping, M. *Chem. - Eur. J.* **2014**, *20*, 13913–13917. (f) Wu, Z.; Harutyunyan, S. R.; Minnaard, A. J. *Chem. - Eur. J.* **2014**, *20*, 14250–14255. (g) Kaib, P. S. J.; List, B. *Synlett* **2016**, *27*, 156–158.

(31) (a) Uyanik, M.; Hayashi, H.; Ishihara, K. *Science* **2014**, *345*, 291–294. (b) Wang, P.-S.; Liu, P.; Zhai, Y.-J.; Lin, H.-C.; Han, Z.-Y.; Gong, L.-Z. *J. Am. Chem. Soc.* **2015**, *137*, 12732–12735.

(32) (a) Liu, K.; Chougnat, A.; Woggon, W.-D. *Angew. Chem., Int. Ed.* **2008**, *47*, 5827–5829. (b) Chougnat, A.; Liu, K.; Woggon, W.-D. *Chimia* **2010**, *64*, 303–308. (c) Ishikawa, T.; Tokunou, S.; Nakanishi, W.; Kagawa, N.; Kumamoto, T. *Heterocycles* **2012**, *84*, 1045–1056.

(33) For recent other examples for asymmetric synthesis of tocopherol, see: (a) Hernandez-Torres, G.; Urbano, A.; Carreño, M. C.; Colobert, F. *Org. Lett.* **2009**, *11*, 4930–4933. (b) Termath, A. O.; Sebode, H.; Schlundt, W.; Stemmler, R. T.; Netscher, T.; Bonrath, W.; Schmalz, H.-G. *Chem. - Eur. J.* **2014**, *20*, 12051–12055.

(34) Ong, W.; Yang, Y.; Cruciano, A. C.; McCarley, R. L. *J. Am. Chem. Soc.* **2008**, *130*, 14739–14744.